Biochemical and Biophysical Research Communications 528 (2020) 499–505

Contents lists available at ScienceDirect

Biochemical and Biophysical Research Communications

journal homepage: www.elsevier.com/locate/ybbrc

Assessment of insulin resistance in the skeletal muscle of mice using positron emission tomography/computed tomography imaging

Yumiko Miyatake [a, 1], Yuna Mishima [a, 1], Rie Tsutsumi [a], Tamaki Otani [b], Naoya Suemasa [a], Saeko Masumoto [a], Masashi Kuroda [a], Hiroshi Sakaue [a, c, *]

[a] Department of Nutrition and Metabolism, Institute of Biomedical Sciences, Tokushima University Graduate School, 3-18-15, Kuramoto-cho, Tokushima City, 770-8503, Tokushima, Japan
[b] Radioisotope Research Center, Tokushima University Graduate School, Tokushima City, Tokushima, 7708503, Japan
[c] Diabetes Therapeutics and Research Center, Institute of Advanced Medical Sciences, Tokushima University, 3-18-15, Kuramoto-cho, Tokushima City, 770-8503, Tokushima, Japan

ARTICLE INFO

Article history:
Received 14 May 2020
Accepted 22 May 2020
Available online 5 June 2020

Keywords:
PET/CT
FDG
Insulin resistance
Skeletal muscle

ABSTRACT

Measuring glucose uptake in the skeletal muscle *in vivo* is an effective method to determine glucose metabolism abnormalities as the skeletal muscle is the principal tissue responsible for glucose disposal and is a major site of peripheral insulin resistance. In this study, we investigated the pathological glucose metabolism dynamics of the skeletal muscle of C57BL/6J mice in a noninvasive and time-sequential manner using positron emission tomography/computed tomography (PET/CT), an imaging technique that uses radioactive substances to visualize and measure metabolic processes in the body, with [^{18}F]-fluoro-2-deoxy-D-glucose (FDG). FDG-PET/CT imaging revealed that insulin administration and exercise load significantly increased FDG accumulation in the skeletal muscle of C57BL/6J mice. FDG accumulation was lower in the skeletal muscle of 14-week-old *db/db* diabetic model mice exhibiting remarkable insulin resistance compared to that of 7-week-old *db/db* mice. Based on the continuous observation of FDG accumulation over time in diet-induced obese (DIO) mice, FDG accumulation significantly decreased in 17-week-old mice after the acquisition of insulin resistance. Although insulin-induced glucose uptake in the skeletal muscle was markedly attenuated in 20-week-old DIO mice that had already developed insulin resistance, exercise load effectively increased FDG uptake in the skeletal muscle. Thus, we successfully confirmed that glucose uptake accompanied by insulin administration and exercise load increased in the skeletal muscle using PET-CT. FDG-PET/CT might be an effective tool that could noninvasively capture the chronological changes of metabolic abnormalities in the skeletal muscle of mice.

List of abbreviations

PET/CT	positron emission tomography/computed tomography
FDG	[^{18}F]-fluoro-2-deoxy-D-glucose
DIO	diet-induced obese
SGLT2	sodium-glucose transport protein 2
VOI	volume of interest
SUV	standardized uptake value
2DG	2-deoxy-D-glucose uptake
ND	normal chow diet

1. Introduction

The skeletal muscle is the largest organ in the body and plays an important role in energy metabolism [1–4]. The glycemic clamp technique, considered as the most common and accurate experimental procedure performed to assess insulin sensitivity *in vivo* [5], showed that the skeletal muscle is generally responsible for insulin-stimulated whole-body glucose disposal [6]. Although this method is the reference standard method performed to directly measure insulin sensitivity [7], we attempted to utilize positron emission tomography/computed tomography (PET/CT), an imaging technique that uses radioactive substances to visualize and measure metabolic processes in the body, with [^{18}F]-fluoro-2-deoxy-D-glucose (FDG) to noninvasively and chronologically observe metabolic changes in the skeletal muscle with the same individual.

* Corresponding author. Department of Nutrition and Metabolism, Institute of Biomedical Sciences, Tokushima University Graduate School, 3-18-15, Kuramoto-cho, Tokushima City, 770-8503, Tokushima, Japan.
E-mail address: hsakaue@tokushima-u.ac.jp (H. Sakaue).
[1] These authors contributed equally to this manuscript.

https://doi.org/10.1016/j.bbrc.2020.05.165
0006-291X/

PET/CT is a widely used examination method that identifies the distribution of tumors by administering substances (e.g., [^{18}F]-fluoro-deoxy-glucose, [^{11}C]-methionine) used as probes for clinical observation [8–10]. Some reports showed that PET/CT can assess the pharmacokinetic properties of different substances, the biodistribution of functional ingredients, and the kinetics of substances that change in diseases such as Alzheimer's disease [11–13]. In the present study, we examined glucose uptake changes in the skeletal muscle of mice based on their insulin resistance using FDG-PET/CT. Additionally, we aimed to establish an observation method of the skeletal muscle's glucose metabolism changes during the development of insulin resistance in mice.

2. Materials and methods

2.1. Animals and experiments

All experiments were approved by the Tokushima University Animal Study Committee and conducted in accordance with the Guidelines for the Care and Use of Animals approved by the Council of the Physiological Society of Japan. All efforts were made to minimize animal suffering and to reduce the number of animals used in the experiments. All mice were housed at a constant room temperature of 23 ± 1 °C with a 12-h light/dark cycle (lights on at 8 a.m.). We purchased 7-week-old C57BL/6J male mice (Japan SLC, Shizuoka, Japan). Mice were fed a standard non-purified diet (Oriental Yeast, Tokyo, Japan) with food and water available *ad libitum*. Mice were divided into three groups: the control group (n = 6), exercise group (n = 6), and intraperitoneal injection group (n = 3). The insulin group received intraperitoneal injection of insulin (1 U/kg Body Weight) after 3-h fasting. All mice immediately received FDG from the tail vein after fasting, and this administered FDG was used for PET imaging (Fig. 1A). Mice in the exercise group performed treadmill exercise (15 m/min, 60 min) during the last hour of fasting (Fig. 1B). Only mice that completed the endurance running were used in this experiment. Furthermore, 6-week-old db/db mice were purchased from Japan SLC (Shizuoka, Japan). After 1 week of adaptation, serum collection and PET imaging were performed in 7-week-old Db/db mice. Moreover, a similar experiment was conducted in 14-week-old db/db mice. To prepare diet-induced obese (DIO) mice, we purchased 4-week-old C57BL/6J male mice (Japan SLC, Shizuoka, Japan). After 1 week of adaptation rearing, mice were provided free access to water and either a control diet (n = 6, 14% of calories from fat [Oriental Yeast Co., Ltd., Tokyo, Japan]) or a high-fat diet (n = 6, 60% of calories from fat [Oriental Yeast Co., Ltd.]) until the mice turned 17 weeks old. Body weight and food intake of each mouse were measured weekly. PET imaging was performed every 2 weeks. When the mice turned 17–20 weeks old, they received an intraperitoneal injection of insulin or exercise load and underwent a PET/CT scan. Additionally, blood glucose level was normalized in the mice model by administering drug. We administered a sodium-glucose transport protein 2 (SGLT2) inhibitor, dapagliflozin (0.1 mg/kg, CS-0781, ChemScene NJ, USA). Blood glucose was measured over time, and PET imaging was performed if the blood glucose level was 200 mg/dl or less at above 4.5 h after the treatment with dapagliflozin(n = 4).

2.2. [^{18}F]-fluoro-2-deoxy-D-glucose-positron emission tomography (FDG-PET)/computed tomography scanning

All scans were performed using a Siemens Inveon small-animal PET/CT scanner (Siemens Healthcare, Knoxville, TN, USA). After measuring the body weight and blood glucose level of mice, we injected 10 MBq/0.1–0.2 mL ^{18}F-FDG via a tail vein catheter. Subsequently, PET was performed for 30 min under inhalation anesthesia (flow rate, 0.6 L/min; concentration, 2%) of isoflurane using an anesthesia machine (anesthesia machine for small-animal SN487-0T Air, Shinano Manufacturing Co., Ltd.). After PET imaging, CT imaging was also performed. During the scan, the temperature was maintained at 28 °C with a heat preservation pad to prevent body temperature drop.

2.3. FDG-PET image analysis

The PET and CT images were analyzed using PMOD software version 3.204 (PMOD Technologies LLC, Zürich, Switzerland). The PET list-mode files were reconstructed for 3 dimensions (3D) ordered-subject expectation maximization followed by maximum a posteriori reconstruction (3D OS-EM/MAP) for static images and absorption correction and scattering correction were not performed. For all PET/CT datasets, the volume of interest (VOI) was defined manually around the hindlimb skeletal muscle, referring to the CT image, and the %ID value was calculated from the fused PET images. The calculation formulas are as follows, with the unit of the PET image being set to a standardized uptake value (SUV) using a software:

$$\%ID/L = 100 \times \text{radioactivity concentration in VOI/injected radioactivity}$$

2.4. Measurement of 2-deoxy-D-glucose uptake

Mice received 5 μmol of 2-deoxyglucose through the tail vein after 3-h fasting. Insulin (1 U/kg Body Weight) was administered, or treadmill exercise (15 m/min, 60 min) was immediately performed. Hindlimb muscles were isolated and used for measurement. The tissues were homogenized with 10 mM Tris-hydrochloride (Tris-HCl) (pH, 8.1). After incubating at 95 °C for 15 min, the sample was centrifuged (17800 g, 4 °C, 15 min), and the supernatant was collected. The supernatant was diluted with the appropriate corresponding concentrations (soleus, 20-fold dilution; extensor digitorum longus; gastrocnemius, 8-fold dilution) and was used for measurement. We used a Glucose Cellular Uptake Measurement Kit (Cosmo Bio Co., Ltd., Japan). An experiment was conducted according to the attached protocol.

2.5. Measurement of serum insulin and calculation of insulin resistance index

Blood samples were obtained from the tail vein. All samples were allowed to naturally clot for 30 min and centrifuged at 3000 rpm for 15 min. The supernatant was collected and stored at -80 °C until analysis. Serum levels of Insulin were measured using the Morinaga Ultra-Sensitive Mouse Insulin ELISA Kit (Morinaga Institute of Biological Science, Yokohama, Japan), according to the manufacturer's recommended protocols. The insulin resistance index was calculated using the following formula: (glucose [mmol/L] × insulin [μU/mL]/22.5), using fasting values [14].

2.6. Immunoblot analysis

Total protein was extracted from the mouse soleus muscle by homogenization in lysis buffer. The lysis buffer (1 M Tris-HCl, 0.1 M Ethylenediaminetetraacetic acid-2Na, 1% Nonidet P-40 $Na_4P_2O_7$, phosphatase inhibitor cocktail Ethylenediaminetetraacetic acid-free [Nacalai, Osaka, Japan], protease inhibitor cocktail [Nacalai, Osaka, Japan]) at 150 μL was added to each sample to extract the protein fraction. A protein assay supernatant (14,500 rpm, 4 °C, centrifuged for 10 min) (Pierce BCA Protein Assay Kit, Thermo

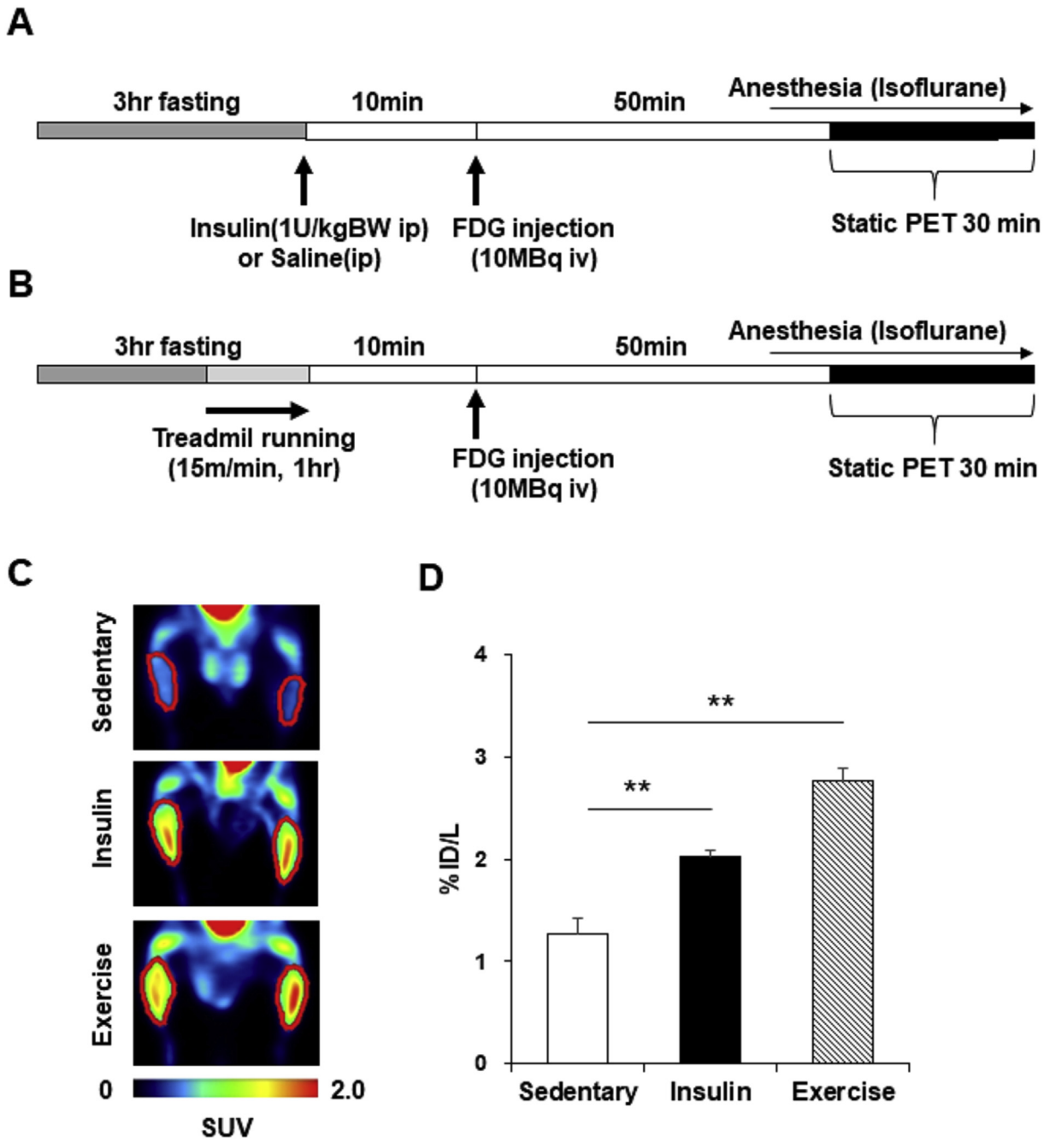

Fig. 1. Workflows for [^{18}F]-fluoro-2-deoxy-D-glucose-positron emission tomography/computed tomography (PET/CT) imaging studies and insulin- and exercise-increased glucose uptake in the skeletal muscle of mice. **(A and B)** The protocol including time points for the start of fasting, injection of insulin (A) or treadmill running (B), injection of ^{18}F-FDG, injection of anesthetics, and PET/CT scan. **(C)** Visual PET images showed each group's hindlimb 7-week-old male C57BL/6J mice that were divided into three groups: sedentary (n = 6), insulin (n = 3), or moderate exercise (n = 6). Red circle indicates regions of interest. The radiation scale is expressed as a standardized uptake value. **(D)** Quantification of radioactivity (%ID/L) in the hindlimb skeletal muscle. Values represent the mean ± standard error of the mean. $^{**}p < 0.01$ vs. the sedentary group.

Fisher Scientific, Waltham, MA) was protein quantified and used for Western blotting. After protein separation by Sodium dodecyl sulfate-polyacrylamide gel electrophoresis on 9%/4% gel was performed, the protein was transferred to polyvinylidene difluoride membrane and blocked at room temperature for 1 h in 5% skim milk. Primary antibodies, including anti-Rabbit P-Akt (Ser473) antibody (CST, Tokyo, Japan), anti-Rabbit Akt antibody (CST, Tokyo, Japan), anti-Rabbit P-p70S6K (Thr389) antibody (CST, Tokyo, Japan), and anti-Rabbit p70S6K antibody (CST, Tokyo, Japan), were used and reacted for 16 h at 4 °C. As a loading control, anti-Rabbit glyceraldehyde 3-phosphate dehydrogenase antibody (Proteintech, Tokyo, Japan) was used. The secondary anti-rabbit horseradish peroxidase labeled antibody (MBL, Nagoya, Japan) was used. Bands obtained by the immune response were detected using the Luminoimage Analyzer Amersham Imager 600 (GE Healthcare UK Ltd., England) and quantified using ImageJ software.

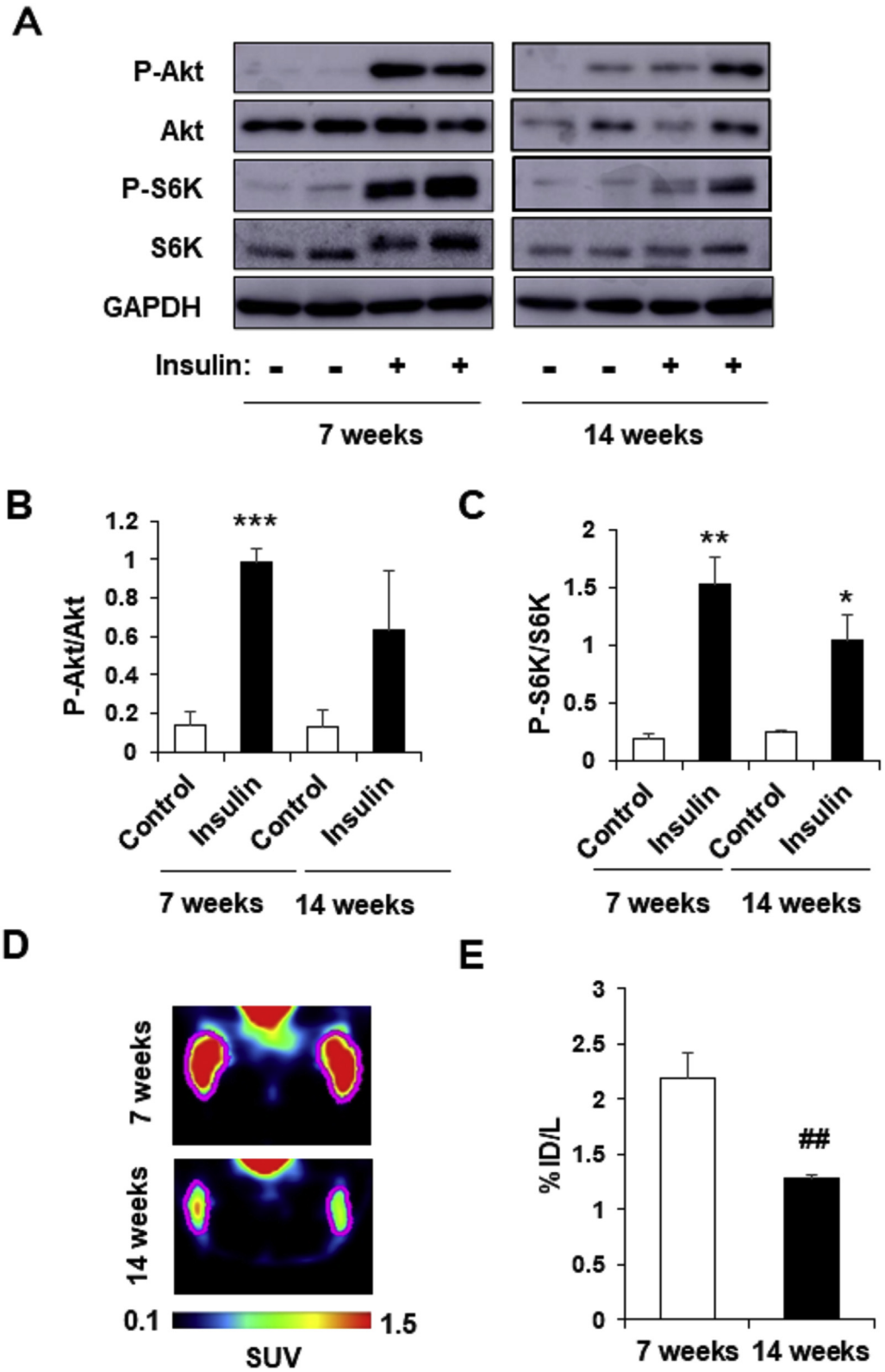

Fig. 2. Reduction of [^{18}F]-fluoro-2-deoxy-D-glucose accumulation in the skeletal muscle in 14-week-old *db/db* mice exhibiting remarkable insulin resistance. **(A–C)** Representative immunoblots (A) and quantification (B–C) of phosphorylated Akt, total Akt, phosphorylated S6K, total S6K, and glyceraldehyde 3-phosphate dehydrogenase in the soleus muscles of control (n = 4) and diet-induced obese (n = 4) mice; saline (control) or insulin was intraperitoneally injected an hour before sacrifice. **(D–E)** Visual positron emission tomography images (D) and quantification of radioactivity (%ID/L) in the hindlimb skeletal muscle (E). Quantify graph showed each group's hindlimb 7-week-old (n = 6) or 14-week-old (n = 6) male *db/db* mice. Red circle indicates regions of interest. The radiation scale is expressed as a standardized uptake value. Values represent the mean ± standard error of the mean. *$p < 0.05$, **$p < 0.01$ vs. the control group, $^{\#\#}p < 0.01$ vs. 7-week-old *db/db* mice group.. (For interpretation of the references to colour in this figure legend, the reader is referred to the Web version of this article.)

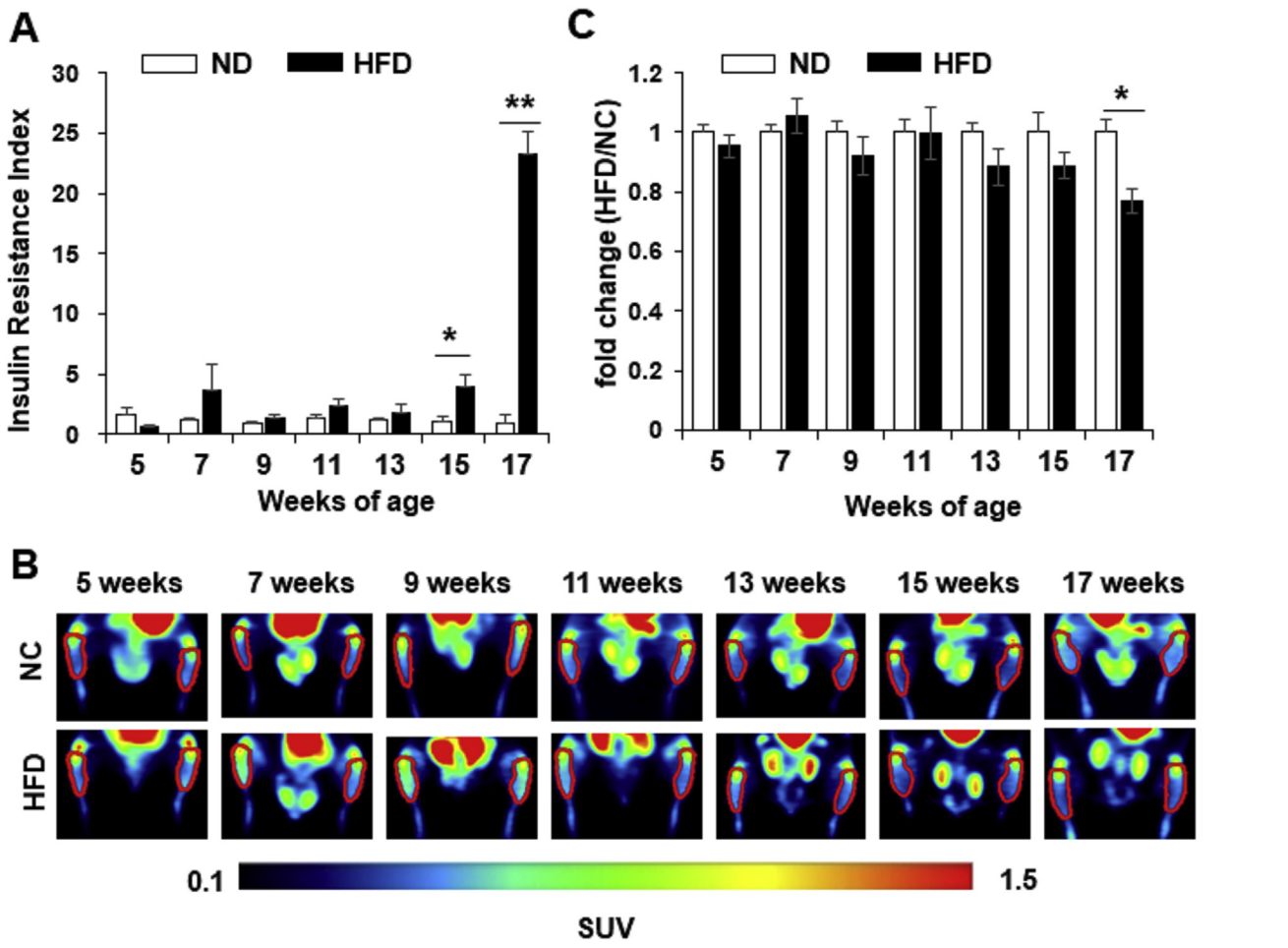

Fig. 3. Long-term high-fat diet (HFD) intake affects glucose uptake in the skeletal muscle. **(A)** The insulin resistance index between normal chow diet (n = 6) and high-fat diet (n = 6) mice (normal chow diet mice, ND: white bar; high-fat diet mice, HFD: black bar). **(B)** Visual positron emission tomography images showed each group's hindlimb, which is ND or HFD mice. Red circle indicates regions of interest. The radiation scale is expressed as a standardized uptake value. **(C)** Comparison of radioactivity (%ID/L) in the hindlimb skeletal muscle between ND and HFD mice. The fold change calculated by dividing the HFD value by the ND value represents the mean ± standard error of the mean. *$p < 0.05$ and **$p < 0.01$ vs. the ND group. (For interpretation of the references to colour in this figure legend, the reader is referred to the Web version of this article.)

2.7. Statistical analyses

Results are expressed as the mean ± standard error of the mean. Data from two groups were analyzed using Student's t-test. Data from more than two groups were analyzed using one-way analysis of variance, followed by the Tukey-Kramer test. P-values <0.05 were considered statistically significant.

3. Results and discussion

3.1. FDG-PET is an effective tool to capture glucose uptake in the skeletal muscle of mice

Intraperitoneal administration of insulin and exercise load increases skeletal muscle glucose uptake [15,16]. We investigated whether the promotion of glucose uptake by these stimuli can be captured by PET/CT with FDG in C57BL/6J mice according to the protocols presented in Fig. 1A and B. Intraperitoneal injection of insulin and exercise load significantly increased FDG accumulation in the hindlimb skeletal muscle of C57BL/6J mice (Fig. 1C and D). Considering that we also administered nonradioactive 2-deoxy-D-glucose (2DG) in the same protocol as in PET imaging (Fig. 1B) and measured the 2DG content of the excised skeletal muscle, similar 2DG uptake was observed in the excised skeletal muscle of C57BL/6J mice (data not shown).

3.2. Reduction of FDG accumulation in the skeletal muscle in 14-week-old db/db mice exhibiting remarkable insulin resistance

We subsequently investigated the FDG uptake of the skeletal muscle in *db/db* mice, described as DIO mice showing hyperglycemia and hyperinsulinemia associated with leptin receptor deficiency [17]. Although serum insulin (18.55 ± 3.45 ng/mL) and blood glucose levels were significantly higher in 7-week-old *db/db* mice compared with those of control *db/ +* mice (6.83 ± 0.20 ng/mL), circulating insulin concentrations spontaneously increased in 14-week old *db/db* mice (56.32 ± 24.51 ng/mL). Glucose uptake in the skeletal muscle is dependent on the translocation of glucose transporter type 4 glucose transporters to the plasma membrane, which is closely regulated by PI3K and Akt signaling in response to insulin treatment [18]. As previously reported by Shoa J et al. [19], insulin-induced Akt or S6K phosphorylation in the skeletal muscle of 14-week-old *db/db* mice was markedly more attenuated compared with those of 7-week-old mice (Fig. 2A–C). The FDG uptake of the skeletal muscle was also significantly inhibited in 14-week-old *db/db* mice despite the presence of hyperinsulinemia (Fig. 2C and D). These data suggest that PET/CT could possibly evaluate the changes in the FDG uptake of the skeletal muscle due

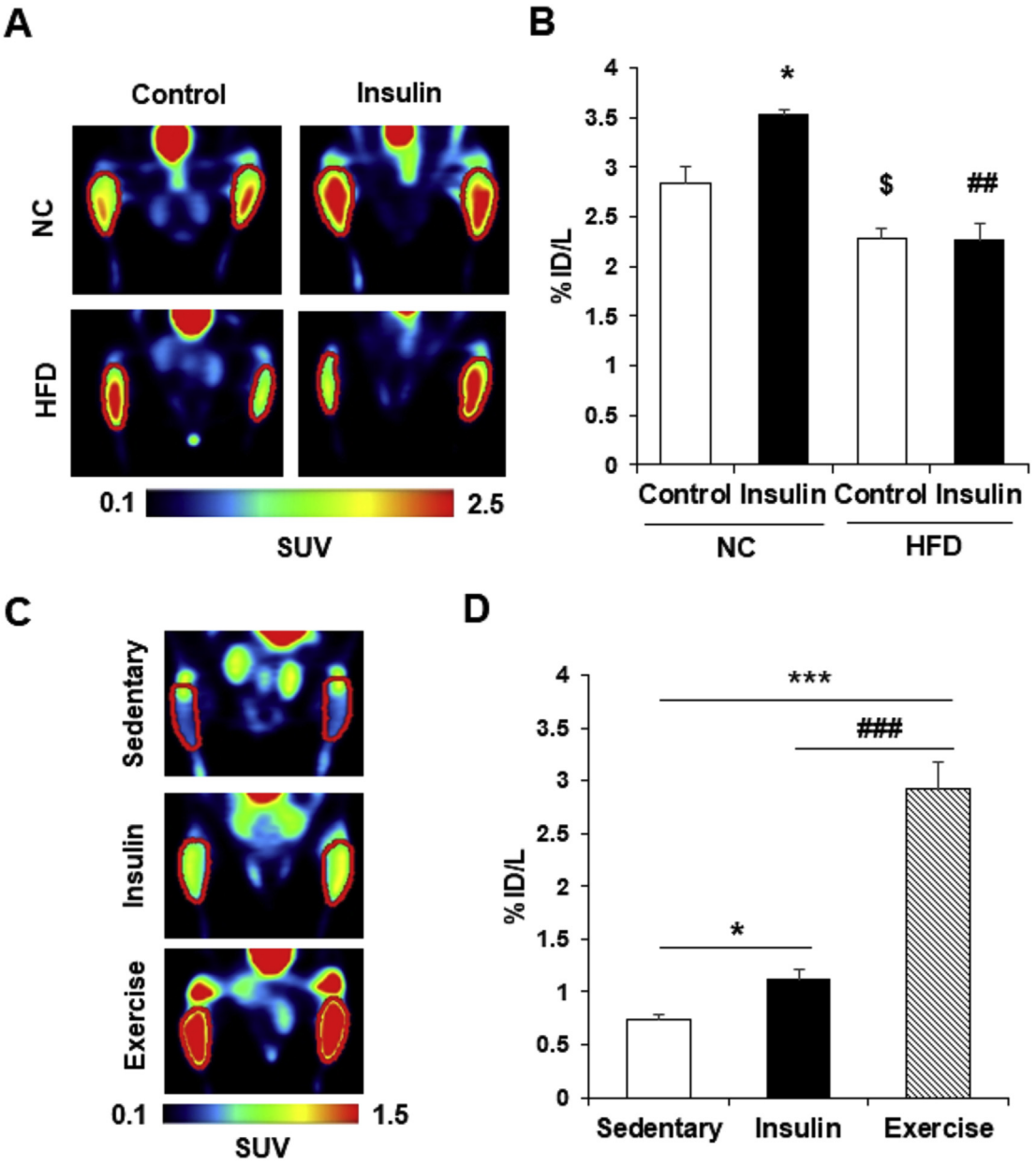

Fig. 4. Effect of exercise on glucose uptake in the skeletal muscle of diet-induced obese (DIO) mice. **(A–B)** Visual positron emission tomography (PET) images (A) and quantification of radioactivity (%ID/L) in the hindlimb skeletal muscle (B). Quantifying graph showed each group's hindlimb control (n = 3) or insulin group (n = 3) of 20-week-old DIO mice. Red circle indicates regions of interest. The radiation scale is expressed as a standardized uptake value. $^{*}p < 0.05$ vs. the control ND group, $^{\#\#}p < 0.01$ vs. the control HFD group, $^{\$}p < 0.05$ the control ND group vs. the control HFD group. **(C–D)** Visual PET images (C) and quantification of radioactivity (%ID/L) in the hindlimb skeletal muscle (D). Quantifying graph showed each group's hindlimb control (n = 6) or exercise group (n = 6) of 17-week-old DIO mice. Values represent the mean ± standard error of the mean. Red circle indicates regions of interest. The radiation scale is expressed as a standardized uptake value. $^{*}p < 0.05$, $^{***}p < 0.001$ vs. sedentary, $^{\#\#\#}p < 0.001$ insulin vs. exercise group. (For interpretation of the references to colour in this figure legend, the reader is referred to the Web version of this article.)

to the differences in the degree of insulin resistance in the same individual.

3.3. Long-term high-fat diet intake affects glucose uptake in the skeletal muscle

To observe a decrease in FDG accumulation in the skeletal muscle due to insulin resistance, we evaluated the glucose uptake of the skeletal muscle in DIO mice. The body weight of DIO mice was higher after these mice turned 11 weeks old compared with that of normal chow diet (ND) mice and significantly increased after the DIO mice turned 17 weeks old (data not shown). Fasting blood glucose levels significantly increased after the DIO mice turned 11 weeks old (data not shown), and serum insulin levels also significantly increased after the DIO mice turned 15 weeks old (data not shown). Based on the insulin resistance index, fasting glucose and insulin levels significantly and markedly increased in 15- and 17-week old DIO mice, respectively (Fig. 3A). FDG accumulation in the skeletal muscle started to decrease in 13-week-old DIO mice, and significant reduction was observed in 17-week-old DIO mice (Fig. 3B and C).

The FDG uptake of the skeletal muscle is well known to be competitively inhibited by blood glucose increase. Therefore, the decrease in the FDG uptake in DIO mice may be associated with

hyperglycemia. To examine the effect of hyperglycemia on glucose uptake, we temporarily corrected the blood glucose level of DIO mice using the SGLT2 inhibitor dapagliflozin [20]. Although fasting blood glucose level decreased from 277.67 ± 17.27 mg/dl to 186.00 ± 15.17 mg/dl with the administration of dapagliflozin in 20-week-old DIO mice, the reduction of glucose uptake was not associated with an ND (data not shown). Thus, the decrease in the skeletal muscle glucose uptake in DIO mice was visualized using FDG-PET/CT independent of blood glucose levels.

3.4. Effect of exercise on glucose uptake in the skeletal muscle of diet-induced obese mice

We finally examined the insulin-induced glucose uptake in the skeletal muscle of 20-week-old DIO mice. At 17–20 weeks of age, serum insulin and blood glucose levels were significantly higher in DIO mice than those in ND mice (data not shown). Although fasting blood glucose levels decreased from 219.33 ± 13.96 mg/dl to 72 ± 10.60 mg/dl and from 309.33 ± 29.18 mg/dl to 79 ± 10.69 mg/dl in 20-week-old NC or DIO mice, respectively, by intraperitoneal administration of insulin (1 U/kg Body Weight), insulin-activated FDG uptake did not increase in DIO mice, but not in ND mice (Fig. 4A and B). Exercise is a relevant stimulator of insulin-independent glucose transport [21]. In 17-week-old DIO mice, FDG accumulation in the skeletal muscle increased by insulin stimulation or moderate exercise load, which was more pronounced in the exercise load than in insulin stimulation (Fig. 4C and D). These results suggest that exercise stimulation can more strongly promote skeletal muscle glucose uptake than insulin stimulation in DIO mice exhibiting insulin resistance.

In this study, we attempted to provide a noninvasive and convenient method of determining skeletal muscle metabolism changes using FDG-PET/CT and successfully established a method used to measure glucose uptake in mouse hindlimb skeletal muscles and observed changes in glucose metabolism in the skeletal muscles of diabetic mice over time. However, these data need to be compared with those obtained with conventional insulin resistance evaluation methods, such as glucose clamping. Additionally, if we use a compartment model in FDG-PET/CT, quantification with higher accuracy becomes possible [22,23].

In conclusion, FDG-PET/CT methods could noninvasively visualize the effect of insulin administration and exercise load on the glucose uptake of the skeletal muscle in insulin resistance mice models. Although exercise therapy is recommended in diabetic patients, data comparing the benefits of exercise therapy with those of insulin therapy are relatively insufficient. The finding that moderate exercise markedly increased the glucose uptake of the skeletal muscle in DIO mice might provide new information about the role of exercise in the prevention of skeletal muscle insulin resistance.

Funding sources

This work was supported by Funds for the Development of Human Resources in Science and Technology under MEXT through the Home for Innovative Researchers and Academic Knowledge Users consortium and KAKENHI Grant (18K16205 to M.K. and 19H04055 to H.S.) from the Japan Society for the Promotion of Science.

Declaration of competing interest

The authors declare that they have no known competing financial interests or personal relationships that could have appeared to influence the work reported in this paper.

Acknowledgment

This study was technically supported by members of the Radioisotope Center of Tokushima University Graduate School and those of RIKEN Center for Life Science Technologies for performing FDG-PET/CT.

References

[1] B.H. Goodpaster, L.M. Sparks, Metabolic flexibility in health and disease, Cell Metabol. 2 (2017) 1027–1036.
[2] J. Aucouturier, P. Duché, B.W. Timmons, Metabolic flexibility and obesity in children and youth, Obes. Rev. 12 (2011) e44–e53.
[3] E. Phielix, M. Mensink, Type 2 diabetes mellitus and skeletal muscle metabolic function, Physiol. Behav. 23 (2008) 252–258.
[4] M.C. Petersen, G.I. Shulman, Mechanisms of insulin action and insulin resistance, Physiol. Rev. 98 (2018) 2133–2223.
[5] R.A. DeFronzo, J.D. Tobin, R. Andres, Glucose clamp technique: a method for quantifying insulin secretion and resistance, Am. J. Physiol. 237 (1979) E214–E223.
[6] R.A. DeFronzo, D. Tripathy, Skeletal muscle insulin resistance is the primary defect in type 2 diabetes, Diabetes Care 32 (2009) S157–S163.
[7] R. Muniyappa, S. Lee, H. Chen, M.J. Quon, Current approaches for assessing insulin sensitivity and resistance in vivo: advantages, limitations, and appropriate usage, Am. J. Physiol. Endocrinol. Metab. 294 (2008) E15–E26.
[8] S. Hess, B.A. Blomberg, H.J. Zhu, P.F. Høilund-Carlsen, A. Alavi, The pivotal role of FDG-PET/CT in modern medicine, Acad. Radiol. 21 (2014) 232–249.
[9] A.W. Glaudemans, R.H. Enting, M.A. Heesters, R.A. Dierckx, R.W. van Rheenen, A.M. Walenkamp, R.H. Slart, Value of 11C-methionine PET in imaging brain tumours and metastases, Eur. J. Nucl. Med. Mol. Imag. 40 (2012) 615–635.
[10] K. Mitamura, Y. Yamamoto, T. Norikane, T. Hatakeyama, M. Okada, Y. Nishiyama, Correlation of 18F-FDG and 11C-methionine uptake on PET/CT with Ki-67 immunohistochemistry in newly diagnosed intracranial meningiomas, Ann. Nucl. Med. 32 (2018) 627–633.
[11] D.J. Donnelly, Small molecule PET tracers in drug discovery, Semin. Nucl. Med. 47 (2017) 454–460.
[12] H. Doi, A. Mawatari, M. Kanazawa, S. Nozaki, Y. Nomura, T. Kitayoshi, K. Akimoto, M. Suzuki, S. Ninomiya, Y. Watanabe, Synthesis of 11C-labeled thiamine and fursultiamine for in vivo molecular imaging of vitamin B1 and its prodrug using positron emission tomography, J. Org. Chem. 80 (2015) 6250–6258.
[13] P. Alongi, D.S. Sardina, R. Coppola, S. Scalisi, V. Puglisi, A. Arnone, G.D. Raimondo, E. Munerati, V. Alaimo, F. Midiri, G. Russo, A. Stefano, R. Giugno, T. Piccoli, M. Midiri, L.M.E. Grimaldi, 18F-florbetaben PET/CT to assess Alzheimer's disease: a new analysis method for regional amyloid quantification, J. Neuroimaging 29 (2019) 383–393.
[14] D.R. Matthews, J.P. Hosker, A.S. Rudenski, B.A. Naylor, D.F. Treacher, R.C. Turner, Homeostasis model assessment: insulin resistance and beta-cell function from fasting plasma glucose and insulin concentrations in man, Diabetologia 28 (1985) 412–419.
[15] H. Yaribeygi, F.R. Farrokhi, A.E. Butler, A. Sahebkar, Insulin resistance: review of the underlying molecular mechanisms, J. Cell. Physiol. 234 (2019) 8152–8161.
[16] L. Sylow, M. Kleinert, E.A. Richter, T.E. Jensen, Exercise-stimulated glucose uptake - regulation and implications for glycaemic control, Nat. Rev. Endocrinol. 13 (2017) 133–148.
[17] H. Kodama, M. Fujita, I. Yamaguchi, Development of hyperglycaemia and insulin resistance in conscious genetically diabetic (C57BL/KsJ-db/db) mice, Diabetologia 37 (1994) 739–744.
[18] L.R. Pearce, D. Komander, D.R. Alessi, The nuts and bolts of AGC protein kinases, Nat. Rev. Mol. Cell Biol. 11 (2010) 9–22.
[19] J. Shao, H. Yamashita, L. Qiao, J.E. Friedman, Decreased Akt kinase activity and insulin resistance in C57BL/KsJ-Leprdb/db mice, J. Endocrinol. 167 (2000) 107–115.
[20] W. Meng, B.A. Ellsworth, A.A. Nirschl, P.J. McCann, M. Patel, R.N. Girotra, G. Wu, P.M. Sher, E.P. Morrison, S.A. Biller, R. Zahler, P.P. Deshpande, A. Pullockaran, D.L. Hagan, N. Morgan, J.R. Taylor, M.T. Obermeier, W.G. Humphreys, A. Khanna, L. Discenza, J.G. Robertson, A. Wang, S. Han, J.R. Wetterau, E.B. Janovitz, O.P. Flint, J.M. Whaley, W.N. Washburn, Discovery of dapagliflozin: a potent, selective renal sodium-dependent glucose cotransporter 2 (SGLT2) inhibitor for the treatment of type 2 diabetes, J. Med. Chem. 51 (2008) 1145–1149.
[21] D.G. Hardie, K. Sakamoto, AMPK: a key sensor of fuel and energy status in skeletal muscle, Physiology (Bethesda) 21 (2006) 48–60.
[22] K.V. Williams, A. Bertoldo, P. Kinahan, C. Cobelli, D.E. Kelley, Weight loss-induced plasticity of glucose transport and phosphorylation in the insulin resistance of obesity and type 2 diabetes, Diabetes 52 (2003) 1619–1626.
[23] S.L. Ménard, E. Croteau, O. Sarrhini, R. Gélinas R, P. Brassard, R. Ouellet, M. Bentourkia, J.E. van Lier, C. Des Rosiers, R. Lecomte, A.C. Carpentier, Abnormal in vivo myocardial energy substrate uptake in diet-induced type 2 diabetic cardiomyopathy in rats, Am. J. Physiol. Endocrinol. Metab. 298 (2010) 1049–1057.